Intermixing at the heterointerface between ZnS/Zn(S,O) bilayer buffer and $CuInS_2$ thin film solar cell absorber

M. Bär[a),b)]
Solarenergieforschung (SE2), Hahn-Meitner-Institut Berlin, Glienicker Strasse 100, D-14109 Berlin, Germany and Department of Chemistry, University of Nevada, Las Vegas, 4505 Maryland Parkway, Box 454003, Las Vegas, Nevada 89154-4003

A. Ennaoui,[a),c)] J. Klaer, T. Kropp, R. Sáez-Araoz, S. Lehmann, A. Grimm, I. Lauermann, Ch. Loreck, St. Sokoll, H.-W. Schock, Ch.-H. Fischer,[d)] and M. C. Lux-Steiner[d)]
Solarenergieforschung (SE2, SE3), Hahn-Meitner-Institut Berlin, Glienicker Strasse 100, D-14109 Berlin, Germany

Ch. Jung
Berliner Elektronenspeicherring-Gesellschaft für Synchrotronstrahlung m.b.H., Albert-Einstein-Strasse 15, 12489 Berlin, Germany

(Received 21 February 2006; accepted 2 July 2006; published online 28 September 2006)

The application of Zn compounds as buffer layers was recently extended to wide-gap $CuInS_2$ (CIS) based thin-film solar cells. Using an alternative chemical deposition route for the buffer preparation aiming at the deposition of a single-layer, nominal ZnS buffer without the need for any toxic reactants such as hydrazine has helped us to achieve a similar efficiency as respective CdS-buffered reference devices. After identifying the deposited Zn compound, as ZnS/Zn(S,O) bilayer buffer in former investigations [M. Bär *et al.*, J. Appl. Phys. **99**, 123503 (2006)], this time the focus lies on potential diffusion/intermixing processes at the buffer/absorber interface possibly, clarifying the effect of the heat treatment, which drastically enhances the device performance of respective final solar cells. The interface formation was investigated by x-ray photoelectron and x-ray excited Auger electron spectroscopy. In addition, photoelectron spectroscopy (PES) measurements were also conducted using tunable monochromatized synchrotron radiation in order to gain depth-resolved information. The buffer side of the buffer/absorber heterointerface was investigated by means of the characterization of Zn(S,O)/ZnS/CIS structures where the ZnS/Zn(S,O) bilayer buffer was deposited successively by different deposition times. In order to make the (in terms of PES information depth) deeply buried absorber side of the buffer/absorber heterointerface accessible for characterization, in these cases the buffer layer was etched away by dilute HCl_{aq}. We found indications that while (out-leached) Cu from the absorber layer forms together with the educts in the chemical bath a $[Zn_{(1-Z)},Cu_{2Z}]$S-like interlayer between buffer and absorber, Zn is incorporated in the uppermost region of the absorber. Both effects are strongly enhanced by postannealing the Zn(S,O)/ZnS/CIS samples. However, it was determined that the major fraction of the Cu and Zn can be found quite close to the heterointerface in the buffer and absorber layer, respectively. Due to this limited (in the range of one monolayer) spatial extent, these "diffusion" mechanisms were rather interpreted as a chemical bath deposition induced and heat-treatment promoted Cu-Zn ion exchange at the buffer/absorber interface. Possible impacts of this intermixing on the performance of the final solar cell devices will also be discussed. © *2006 American Institute of Physics*.
[DOI: 10.1063/1.2345034]

I. INTRODUCTION

Chalcopyrite solar cells based on the $Cu(In_{1-X}Ga_X)(S_YSe_{1-Y})_2$ (CIGSSe) material system are the most promising among thin-film photovoltaic devices. Laboratory-scale (active area=0.41 cm^2) prototypes with a device structure as simple as n^+-ZnO/*i*-ZnO/buffer/CIGSSe/Mo/glass reach already efficiencies (η) close to 20% if a combination of a low-gap ($E_g \approx 1.15$ eV) S-free chalcopyrite absorber ($Cu(In,Ga)Se_2$, "CIGSe") and wet-chemically-—in a chemical bath (CBD)—deposited CdS buffer layer is applied.[2,3] In the recent past, because of the toxicity and the low transparency in the blue wavelength region of the CBD-CdS buffer, there were many efforts to replace the CdS layer with different (CBD) Zn–S compounds, denoted by the respective authors as ZnS,[4] Zn(S,OH),[5–7] ZnS(O,OH),[8,9] $Zn(O,S,OH)_x$,[10] and $ZnS_xO_yH_z$.[11] However, despite of a higher transparency and thus a higher current collection in the blue wavelength region the direct comparison of devices based on world record CIGSe absorber material from the National Renewable Energy Laboratory (NREL) (Golden, CO, USA) with Zn–S compound buffer layers [η_{max}(Zn–S)=18.6% (Ref. 9)]

[a)]Authors to whom correspondence should be addressed.
[b)]FAX: 1-702-895-4072; electronic mail: baerm2@unly.nevada.edu
[c)]FAX: +49-(0)30-8062-3199; electronic mail: ennaoui@hmi.de
[d)]Also at Freie Universität Berlin, 14195 Berlin, Germany.

with the respective CBD-CdS buffered CIGSe-based solar cell references [$\eta_{max}(CdS)=19.5\%$ (Ref. 2)] shows an efficiency gap of ~1% (abs.). (Note that these η values are based on the *active area* of the solar cell.) Recently, this efficiency gap could be closed for production scale low-gap $Cu(In,Ga)(S,Se)_2$ absorbers provided by Shell Solar GmbH (Munich, Germany) applying CBD-Zn-compound buffer layers developed at the Hahn-Meitner-Institut Berlin (HMI) (Berlin, Germany).[5–7] In this case, the obtained *total area* device efficiency [$\eta_{max}(Zn-S)=14.4\%$) was comparable to that of corresponding CBD-CdS buffered references [$\eta_{max}(CdS)=14.6\%$]—independently confirmed by NREL.[7]

However, when transferring this approach to wide-gap ($E_g=1.54$ eV) $CuInS_2$ (CIS) based devices—which, according to theoretical considerations,[12] promise a higher efficiency than the current low-gap world record chalcopyrite solar cell and are additionally of particular interest in terms of a possible application as top cell in a prospective chalcopyrite tandem cell—resulting devices with CBD-$ZnS_xO_yH_z$ buffers have yielded *active area* efficiencies of up to 10.7%,[11] whereas corresponding CBD-CdS buffered references reached 11.9%, again showing the efficiency gap of ~1% (abs.).

Recent additional efforts initially aiming at a single-layer, nominal ZnS buffer CBD process without the need of any toxic reactants such as, hydrazine have helped us to close the efficiency gap between corresponding Cd-free CIS solar cells with Zn-compound buffer layers and standard CdS-buffered reference devices. Resulting CIS-based solar cells with a Zn-compound buffer deposited by this alternative chemical deposition route yielded comparable *total area* efficiencies (10.3%) than CdS-buffered references (10.4%).[13]

Preceding experiments[1] have shown that the deposited nominal ZnS buffer is actually a ZnS/Zn(S,O) bilayer with a thickness dependent ZnS/(ZnS+ZnO)—ratio of ~1 close to the interface with the CIS absorber and ~0.8 at the surface of a thick (>5.4 nm) buffer layer. However, the high efficiencies of CIS-based devices with these buffers are only reached if, subsequently to the buffer preparation and prior to the deposition of the n^+-ZnO/*i*-ZnO window bilayer, the Zn(S,O)/ZnS/CIS/Mo/glass structure is annealed in air (5 min at 200 °C). Due to the hydroxide-poor composition of the ZnS/Zn(S,O) bilayer buffer, which is contrary to the composition of the other Zn–S compound buffers,[5–11] we have found no major change in buffer composition resulting from this postannealing.[1] Whether the improvement of the buffer material's crystalline structure (as shown in Ref. 14) is thus the only possible impact of the heat treatment which can explain the drastic performance enhancement of respective photovoltaic devices or whether the postannealing induces/activates (beneficial?) intermixing and/or diffusion processes along the buffer/absorber interface [as observed at the $CdS/Cu(In,Ga)Se_2$ interface[15]] is subject of this publication.

II. EXPERIMENT

A. Preparation

1. $CuInS_2$ absorber

The CIS absorbers used in this study were prepared in the Technology Department of the HMI by sputter depositing the metallic In and Cu precursor layers on to Mo/glass substrates and subsequent sulfurization by rapid thermal processing using an excess of elemental sulfur vapor. More details on the preparation conditions are described in Ref. 16. Before depositing the ZnS/Zn(S,O) bilayer buffer, an additional etching step in a KCN-containing aqueous solution (KCN_{aq} [3.5%]) was performed to remove Cu_xS segregations. After KCN etching the absorbers are then immediately stored in an aqueous solution containing ammonia ($NH_{3,aq}$ [2.5%]) prior to the buffer preparation.

2. ZnS/Zn(S,O) bilayer buffer

For the preparation of the Zn-compound buffer layer, we used an alternative CBD process, recently developed at the HMI Berlin.[17] The ZnS/Zn(S,O) layers for the samples used in this investigation were deposited onto the KCN-etched CIS/Mo/glass substrates during 3–20 min in the chemical bath. In addition, some buffer/Mo/glass samples were prepared as references. In these cases, the buffer was deposited over a period of 35 min. (A more detailed description of the alternative CBD process can be found in Refs. 13, 14, 17, and 18.) Note that for a ZnS/Zn(S,O) buffer layer deposited during 13.5 min on a CIS absorber a thickness of ~15 nm was reported in Ref. 18. After taking the buffer/CIS samples out of the chemical bath, they were washed in $NH_{3,aq}$ [2.5%] solution in order to avoid an uncontrolled precipitation of $Zn(OH)_2$. In order to minimize contamination from ambient air, the samples were sealed in a polyethylene bag filled with N_2 immediately after preparation (which was done in air). Then, the samples were transferred into the analysis chamber of a combined ultrahigh vacuum (UHV) preparation and spectroscopy system (CISSY, see Ref. 19 for more details) at a base pressure of $<1\times10^{-9}$ mbar via an attached N_2 filled glovebox. In the latter, the samples (usually $\frac{1}{2}\times2$ in.^{2} in dimension) were cut into two pieces from which one was annealed in system and thus in UHV at ~200 °C for 5 min before characterization.

3. Buffer removal by HCl etching

After initial characterization of those "as-prepared" and "postannealed" samples the buffer was removed by etching the sample in 100 ml (HCl_{aq} [5%]) in order to get access to the otherwise—in terms of information depth of the used characterization techniques—deeply buried Zn(S,O)/ZnS/CIS interface. Recently, this procedure was proven to provide plausible results by Liao and Rocket,[20] since the CIS is HCl resistant. Thus, we have etched the buffer/CIS samples by means of various cycles, some of them performed subsequently (15 min, 36 h, and 36 h+45 h=81 h). After each etching step the samples were characterized. Note that the 15 min etching time is actually the sum of three 5 min cycles each performed with fresh etching solution in order to minimize that traces of buffer material already dissolved in the etch solution remain on the sample when taking it out of the HCl_{aq} [5%] solution. Subsequently, the etched samples were rinsed (three times for 1 min) in 100 ml fresh de-ionized water. Furthermore, each sample was finally rinsed under running deionized water (~100ml) dispensed from a wash-

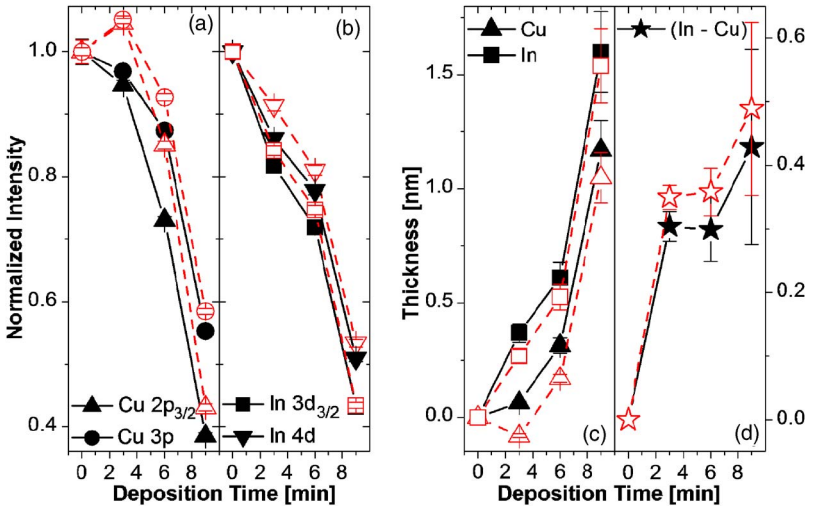

FIG. 1. (Color online) Evolution of the XPS line intensities of the CIS absorber substrate elements Cu (a) and In (b) as a function of the deposition time of the ZnS/Zn(S,O) bilayer buffer normalized to the intensity of the uncovered CIS absorber substrate (0 min). The determined average buffer layer thickness calculated from the In (In $3d_{3/2}$ and In $4d$) and Cu (Cu $2p_{3/2}$ and Cu$3p$) photoemission lines assuming that a pure ZnS layer covers the CIS absorber homogeneously (c) as well as their difference (d) is additionally presented. In addition to the situation of the as-prepared samples (black, solid connection lines, and solid symbols) also that of the postannealed samples (red, dashed connection lines, and open symbols) is shown.

ing bottle and subsequently dried in a nitrogen flow. This entire procedure was also applied for the 36 and 81 h etching cycles as "rinsing mode."

In addition to the buffer/absorber samples, uncovered CIS absorber references were also subject to the applied etching procedures and initial as well as subsequent characterization in order to monitor potential alterations of the absorber's surface.

B. Characterization

The samples were characterized by x-ray photoelectron spectroscopy (XPS) and x-ray excited Auger electron spectroscopy (XAES) using a Mg $K\alpha$ x-ray source (1253.56 eV) and a CLAM4 electron spectrometer from Thermo VG Scientific [calibrated according to Ref. 21 using XPS and Auger line positions of different metals (Cu $3p$, Au $4f_{7/2}$, Cu L_3MM, and Cu $2p_{3/2}$)]. The angle between the sample normal and electron spectrometer (emission angle) φ was in this setup $\sim 0°$.

In addition, we have also performed photoelectron spectroscopy (PES) measurements on the etched samples using tunable monochromatized synchrotron radiation (BESSY II, undulator beamline U41-PGM). In this case, the excitation intensity was also recorded for normalization purposes and the zero point of the energy scale was adjusted for each excitation energy ($h\nu$=174, 224, 274, 374, 454 eV) used, such that the Au $4f_{7/2}$ reference line appears at a binding energy of 84.00 eV.[21] For the synchrotron measurements φ was $\sim 45°$.

For quantitative analysis, we fitted the photoemission signals by Voigt functions. Note that our fit procedure included also a linear background. The intensities of the Au $4f_{7/2}$ photoemission line of the Au reference measured at the synchrotron for different excitation energies were used to determine the transmission function [$\propto$(kinetic energy)$^{-2}$] of the electron analyzer. In order to estimate the thickness of the buffer layer, we used the attenuation of the CIS substrate signals by the increasingly thick buffer, applying Eq. (1),

$$I = I_0 e^{d/\lambda}, \tag{1}$$

where I is the intensity of the respective (attenuated) photoemission signal, I_0 is the unattenuated signal intensity of the bare (KCN-etched) CIS substrate, λ is the escape depth [=inelastic mean free path (IMFP)$\times\cos\varphi$] of the corresponding photoelectrons, and d is the thickness of the attenuating buffer layer. IMFP was calculated by the TPP-2 formula[22] using the QUASES code written by Tougaard,[23] which provides values with an absolute uncertainty of $\sim 10\%$.[23]

III. RESULTS AND DISCUSSION

In order to shed light on possible intermixing/diffusion processes on the buffer side of the Zn(S,O)/ZnS/CIS interface we firstly had a closer look at the buffer/absorber structures, where the samples were taken out of the chemical bath after different times, which were already investigated in Ref. 1 in terms of deposition time and thus thickness-dependent buffer composition. (Note that here intermixing means a spatially limited incorporation of components of the uppermost region of the absorber into the interface-near region of the buffer, whereas diffusion stands for a migration of absorber elements far into the "bulk" of the buffer.) Figure 1 shows the evolution of the XPS line intensities of the CIS absorber substrate elements Cu [Cu $2p_{3/2}$ (triangle) and Cu $3p$ (circle), in Fig. 1(a)] and In [In $3d_{3/2}$ (square) and In $4d$ (inverse triangle), Fig. 1(b)] as a function of the deposition time of the ZnS/Zn(S,O) buffer layer normalized to the intensity of the uncovered CIS absorber substrate (0 min) before (black, solid connection lines) and after (red, dashed connection lines) postannealing. (Note that the intensities of the Cu $3p$ and In $4d$ XPS signals were determined by fitting the corresponding photoemission lines by a doublet of two Voigt functions.) The overall trend of a decrease of the absorber substrate signal intensities with increasing deposition time can be observed before as well as after the postannealing for all substrate signals. It is apparently caused by an increasing attenuation of the absorber substrate XPS lines by the increasing thickness of the growing ZnS/Zn(S,O) buffer layer with deposition time. Note that for a deposition time of

13.5 min no CIS signals can be observed anymore, pointing to a closed ZnS/Zn(S,O) buffer covering the absorber completely with a layer thickness larger than the XPS information depth. As already discussed in Ref. 1 the latter is considered to be three times the inelastic mean free path of the respective photoelectrons[21] (accounting for an attenuation of 95% of the initial intensity) and thus is energy dependent. Assuming that, e.g., the In $3d_{5/2}$ ($E_B \approx 444$ eV) photoelectrons were exclusively attenuated by a pure ZnS layer, which covers the CIS absorber homogeneously, one can estimate the information depth to be 5.4 ± 0.6 nm (based on the IMFP taken from Ref. 23).

In order to analyze now more in detail these data, we first looked at the attenuation behavior of the Cu and In XPS lines for the as-prepared samples. One can observe that the intensities of the Cu $3p$ as well as of the In $4d$ line decrease not as fast with deposition time as the intensities of the Cu $2p_{3/2}$ and In $3d_{3/2}$ XPS signals. This can be attributed to the different IMFPs of the respective photoelectrons. Using the QUASES code written by Tougaard,[23] which is based on the TPP-2 formula,[22] and assuming that the photoelectrons are attenuated by a pure ZnS layer homogeneously covering the CIS absorber, we determined the IMFPs as follows: IMFP (Cu $2p_{3/2}$)=0.96 nm, IMFP (In $3d_{3/2}$)=1.80 nm, IMFP (Cu $3p$)=2.41 nm, and IMFP (In $4d$)=2.50 nm. (Note that these values have an uncertainty of $\sim \pm 10\%$.[23]) The larger IMFPs for Cu $3p$ and In $4d$ compared to those of the Cu $2p_{3/2}$ and In $3d_{3/2}$ photoelectrons, respectively, explain the observed difference in the attenuation behavior of the corresponding XPS line intensities in Figs. 1(a) and 1(b). In addition, we find that because of its small IMFP the Cu $2p_{3/2}$ signal should be attenuated the most among all considered XPS lines. However, comparing the intensity of the Cu $2p_{3/2}$ XPS signal directly with that of the In $3d_{3/2}$ photoemission line, one can observe that the intensity of the In $3d_{3/2}$ XPS line is initially (i.e., for low deposition times and thus for thin buffer layers) lower than the Cu $2p_{3/2}$ intensity. This observation is reversed not until the deposition time of the ZnS/Zn(S,O) buffer exceeds 6 min. This behavior is even more pronounced for the intensities of the Cu $3p$ and In $4d$ XPS lines. Because their IMFPs are almost the same, the intensity ratio of the Cu $3p$ and In $4d$ photoemission lines is even higher than the Cu $2p_{3/2}$/In $3d_{5/2}$ ratio, especially for increasingly thick ZnS/Zn(S,O) buffers. However, in order to include the impact of the IMFP into our considerations, we calculated the thickness of the ZnS/Zn(S,O) buffer based on the attenuation behavior of the Cu and In photoemission lines, assuming again that a pure ZnS buffer layer covers the CIS absorber homogeneously. The determined average buffer layer thickness calculated from the Cu (Cu $2p_{3/2}$ and Cu$3p$) and In (In $3d_{3/2}$ and In $4d$) photoemission lines is shown in Fig. 1(c) as solid triangles and squares, respectively. As already assumed from the deposition time dependent Cu and In XPS line intensities [Figs. 1(a) and 1(b)], it can be observed that the thickness calculated from the attenuation of the In photoemission lines is bigger than that determined from the intensity behavior of the Cu XPS signals. However, the ratio of the thicknesses determined based on the attenuation of the In and Cu photoemission lines, respectively, decreases with increasing buffer deposition time, which shows that the [Cu]/[In] ratio is apparently increasing with increasing duration of the sample in the chemical bath solution. A similar increase of the [Cu]/[In] ratio was observed for (presumably oxidized) $CuInSe_2$ samples, which were immersed in (pure) $NH_{3,aq}$ for an increasing period of time.[24] This could either be explained by the removal of the absorber's surface oxidation (e.g., In_2O_3) by the aqueous ammonia or by an $NH_{3,aq}$-induced leaching out of In as actually suggested in Ref. 24. The latter could, in fact, explain also our finding, since the deposition of the ZnS/Zn(S,O) bilayer buffer takes place in a $ZnSO_4 + SC(NH_2)_2 + NH_{3,aq}$ solution.[13,14,17,18] However, we exclude this explanation in our case because the chemical driving force for this selective etching process is by far lower for the chemical bath solution considered here, since most of the ammonia is already bound in respective complexes (e.g., $[Zn(NH_3)_n]^{+2}$), and hence in this sense only a small amount of the ammonia is actually reactive. Furthermore, the surface etching by $NH_{3,aq}$ and the deposition of the buffer layer are competitive processes,[25] meaning that as soon as the absorber is completely covered by (at least) a monolayer of the buffer material, no more etching of the absorber's surface can take place. In Ref. 1 it was shown that already after a deposition time of 3 min a ZnS layer of $\sim$0.4 nm in thickness is deposited, which corresponds quite well with a dimension of a respective monolayer [0.4–0.6 nm (Ref. 26)]. However, we even expect the ZnS monolayer to be formed almost immediately after immersing the absorber into the CBD solution preventing the absorber surface from being further exposed to the selectively etching $NH_{3,aq}$. This is supported by our recent x-ray emission spectroscopy measurements showing that already after 30 s in a chemical bath (intended to deposit a CdS layer) a significant amount of Cd is found on a CIS absorber.[27] In consequence, the observed different attenuation of the Cu and In XPS signals by the buffer layer can yet only be interpreted as an In migration away from the buffer/absorber interface during ZnS/Zn(S,O) deposition, a Cu migration towards the heterocontact, or even a Cu diffusion out of the CIS into the deposited buffer layer. Regarding the latter two suggestions different statements can be found in the literature. While for the CdS/Cu_2S heterojunction the Cu outdiffusion is a well-known phenomenon,[28,29] for the buffer/CIGSSe heterocontact this was never observed and even ruled out due to the significant built-in potential drop across the space charge region (SCR) in the CIGSSe absorber.[30] Furthermore, the downward surface band bending observed for state-of-the-art CIGSSe absorbers,[31–34] which is believed to be caused by positive surface charges, might induce a Cu "electromigration" away from the buffer/absorber interface.[35,36] However, for the CBD-CdS buffer preparation on CIGSSe absorbers it was repeatedly reported in the past that Cu ions were found in used chemical baths,[37] which were obviously leached out of the absorber's surface as long as the buffer was not completely closed and hence must have taken place in the early stages of the CBD. Altogether we believe that Cu, which is leached out of the absorber's surface (chemically driven by the chemical bath solution) and subsequently is immediately incorporated into the first monolayer(s) of the forming

buffer, explains our findings best. Immediately means here as long as the outleached Cu is still close enough to the CIS surface, i.e., before any noteworthy dilution in the CBD solution can take place. Thus the Cu is not diffusing into the buffer layer, but might rather form together with the educts in the chemical bath a mixture of Cu_2S and ZnS or even a new compound, such as $[Zn_{(1-Z)},Cu_{2Z}]S$. In any case, we will refer to this *interlayer* formed between buffer and absorber as $[Zn_{(1-Z)},Cu_{2Z}]S$-like compound.

Under the assumption that the In XPS signals represent the absorber surface, i.e., there are no intermixing, diffusion, or leaching out processes taking place where In is involved, the difference of the thicknesses determined based on the attenuation of the In and Cu photoemission line attenuation as shown in Fig. 1(d) visualizes the spatial extent of the Cu incorporation into the ZnS/Zn(S,O) bilayer buffer. We find that the spatial Cu extension into the buffer or rather the thickness of the Cu-containing interlayer (between buffer and absorber), which is formed together with the educts of the chemical bath, is 0.34 ± 0.08 nm [average of all three values shown in Fig. 1(d)]. This is in the range of the dimension of a monolayer (see above), which makes absolutely sense, since the Cu out-leaching process will stop immediately once the buffer and interlayer, respectively, cover the CIS completely. Thus, this intermixing process is rather limited to the near buffer/absorber interface region.

The same data, but after postannealing the samples (5 min at ~200 °C in UHV) and recharacterization by XPS, are also shown in Figs. 1(a)–1(d) in red, dashed lines, and open symbols. It can be observed that for all considered photoemission lines the decrease of the XPS signal intensity with deposition time is less pronounced. Besides the trivial explanation (desorption of any surface contamination layer from the samples) this can be explained by a thinner buffer layer after the postannealing or heat-treatment induced/enhanced (additional) diffusion/intermixing processes involving both Cu and In. Altogether, the observed changes in the deposition time dependent intensity behavior after postannealing are probably caused by a superposition of all those "explanations." However, the Cu $2p_{3/2}$ XPS line intensity is again higher for all deposition times compared to that of the In $3d_{3/2}$ photoemission signal, despite of a smaller IMFP (see above). The same is true, and, due to similar IMFPs, even more pronounced for the Cu $3p$ and In $4d$ XPS signal intensities. The average buffer layer thicknesses after postannealing determined according to Eq. (1), based on the attenuation of the Cu and In photoemission lines, are shown in Fig. 1(c). In correspondence to the less pronounced absorber signal attenuation with deposition time also the calculated thicknesses are smaller compared to the values before heat treatment. Nevertheless, we find again that the thickness of the layer covering the CIS absorber calculated from the attenuation of the In photoemission lines is larger compared to that based on the deposition time dependent decrease of the Cu XPS signals. For the as-prepared samples this was interpreted as the formation of a $[Zn_{(1-Z)},Cu_{2Z}]S$-like interlayer between buffer and absorber (see above). Looking at the difference of the thicknesses obtained from the Cu and In XPS line attenuations, respectively, in Fig. 1(d) one can observe that the thickness of the $[Zn_{(1-Z)},Cu_{2Z}]S$-like interlayer is quite similar but exceeds that determined for the as-prepared samples. This tendency {thicker $[Zn_{(1-Z)},Cu_{2Z}]S$-like interlayer after postannealing} might be weakened by diffusion/intermixing processes involving In, which could also be triggered by the heat treatment, since it would foil the usage of the In signal as proper reference for the CIS absorber surface. For example, an additional (temperature driven) In diffusion out of the absorber into the covering buffer layer [as reported for $Cu(In,Ga)(S,Se)_2$ absorbers and ZnSe buffer layers in the past[38,39]] would decrease the determined thickness of the $[Zn_{(1-Z)},Cu_{2Z}]S$-like interlayer [shown in Fig. 1(d)], compared to its "true" dimension.

Anyway, for the postannealed Zn(S,O)/ZnS/CIS samples we observe that the Cu XPS signal intensities are (for a buffer deposition time of 3 min) higher compared to the corresponding photoemission line intensities of the uncovered (KCN-etched) absorber reference [0 min, see Fig. 1(a)]. Even more, the intensities of the Cu $2p_{3/2}$ and the Cu $3p$ photoemission line are roughly the same (contrary to the respective In signals) indicating that there is almost no attenuation of the Cu XPS signals by a coverlayer anymore. According to our thesis from above that (out-leached) Cu forms together with the deposited Zn and S a $[Zn_{(1-Z)},Cu_{2Z}]S$-like compound this can be interpreted as a conversion of the entire "3 min" buffer layer into $[Zn_{(1-Z)},Cu_{2Z}]S$. Thus, the normalized Cu intensity >1 of the postannealed 3 min sample [and the consequential thickness <0 nm for the postannealed 3 min buffer layer, see Fig. 1(d)] can simply be explained by the respective heat-treatment induced enhancement of the Cu content in the uppermost region of the sample. Under the assumption that the thickness of the measured (in terms of composition homogeneously distributed) material corresponds to the XPS information depth, the Cu content for a $[Zn_{(1-Z)},Cu_{2Z}]S$ composition of $Z>2/7$ becomes thus higher than that of $CuInS_2$. However, since the thickness of the $[Zn_{(1-Z)},Cu_{2Z}]S$-like interlayer is smaller than the corresponding XPS information depth (see above), the true Z value is likely much larger. Since the heat treatment takes place in UHV here the underlying mechanism for the conversion of the entire 3 min buffer into the $[Zn_{(1-Z)},Cu_{2Z}]S$ compound must be different from that of the actual formation of the $[Zn_{(1-Z)},Cu_{2Z}]S$-like interlayer in the chemical bath. Possible options include a heat-treatment induced migration of Cu from the absorber bulk towards the buffer/absorber interface filling the liberated Cu sites left behind from the out-leached Cu or a even a "direct" diffusion of Cu into the $[Zn_{(1-Z)},Cu_{2Z}]S$-like interlayer straightly changing the Z composition. The latter mechanism points to a related intermixing process involving Zn.

Thus, in order to shed light on possible intermixing processes on the absorber side of the Zn(S,O)/ZnS/*interlayer*/CIS interface; we etched away the covering layers to get access to the otherwise (in terms of photoelectron spectroscopy information depth) deeply buried buffer/absorber interface. We documented the etching process by means of the most prominent XPS feature of the

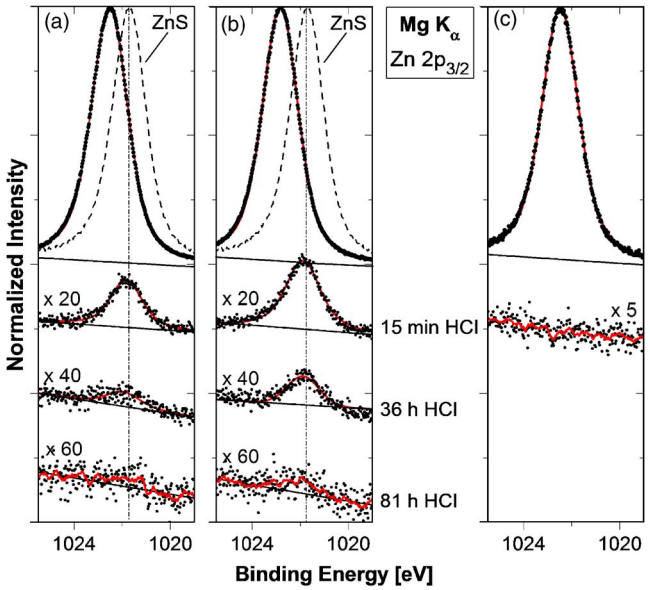

FIG. 2. (Color online) Zn $2p_{3/2}$ photoemission lines of as-prepared (a) and postannealed Zn(S,O)/ZnS/CIS samples (b) as well as of a buffer/Mo reference sample (c) before (uppermost spectra) and after various etching cycles. The dots represent the experimental data and the solid (red) lines the corresponding fits. For the 81 h etched buffer/absorber samples as well as for the 15 min etched buffer/Mo reference reasonably smoothed data are displayed, respectively. In addition, a spectrum of a ZnS reference (dashed lines) is shown as comparison to that of the thick ZnS/Zn(S,O) buffer layers on CIS before etching.

ZnS/Zn(S,O) bilayer buffer, the Zn $2p_{3/2}$ photoemission line as shown in Figs. 2(a) and 2(b) for as-prepared and postannealed Zn(S,O)/ZnS/CIS samples, respectively, as well as in Fig. 2(c) for a buffer/Mo reference sample. The latter is assumed to serve as reference in terms of the progress of the buffer removal by the etching procedure. The figures show the Zn $2p_{3/2}$ XPS signal of thick Zn(S,O)/ZnS/CIS samples before (uppermost spectra) and after 15 min, 36 h, and 81 h HCl_{aq} etching. (For the buffer/Mo reference sample only the spectrum after 15 min HCl_{aq} etching is shown.) Note that the spectra of the etched samples are drawn to a larger scale. The dots represent the experimental data and the solid (red) lines show the corresponding fits by Voigt functions and for the spectra of the Zn(S,O)/ZnS/CIS samples after 81 h HCl_{aq} etching as well as of the buffer/Mo reference sample after 15 min HCl_{aq} etching the reasonably smoothed data, respectively. It can be observed that the intensity of the Zn $2p_{3/2}$ photoemission line for the buffer/absorber samples is drastically reduced already after 15 min HCl_{aq} etching. Interestingly, at the same time the Zn $2p_{3/2}$ XPS signal of the buffer/Mo reference sample vanishes completely, which is assumed to be indicative for the removal of ZnS/Zn(S,O) bilayer buffer also from the CIS absorber. Since we took great care in thoroughly rinsing the samples after the etching steps (see Sec. II), and thus it is unlikely that already dissolved buffer components remain on the sample during emersion the samples out of the HCl_{aq} solution cause the observed Zn $2p_{3/2}$ XPS signals, we interpret this as a Zn incorporation into the CIS absorber. This is also supported by the fact that, in contrast to the otherwise good solubility of ZnS in HCl,[40] one can observe distinct Zn $2p_{3/2}$ XPS signals for the Zn(S,O)/ZnS/CIS samples even after an extended etching of 36 h in HCl_{aq}. {Note that also Cu_2S (Ref. 36) and hence probably also $[Zn_{(1-Z)},Cu_{2Z}]S$ is soluble in HCl and thus also the interlayer is not expected to stay on the CIS after HCl_{aq} etching.} Comparing the as-prepared and postannealed buffer/absorber samples, one can see that for the postannealed samples the signal intensity of the Zn $2p_{3/2}$ photoemission line is consistently larger. Even after HCl_{aq} etching for as long as 81 h, one still might see traces of Zn on the postannealed Zn(S,O)/ZnS/CIS sample, which is in contrast to the situation observed for the as-prepared buffer/absorber sample. Based on the as-prepared samples, we find on average $(61\pm15)\%$ more Zn on the etched postannealed samples. In consequence, the heat treatment apparently enhances the Zn incorporation into the CIS absorber just like it promotes the Cu diffusion out of the CIS into the $[Zn_{(1-Z)},Cu_{2Z}]S$-like interlayer and the buffer layer, respectively, as suggested above.

In order to determine how the Zn is incorporated in the CIS absorber, we looked at the energetic position of the Zn $2p_{3/2}$ photoemission lines, which shifts from a binding energy E_B of 1022.7 ± 0.2 eV for the thick (as-prepared and postannealed) ZnS/Zn(S,O) layers to $E_B=1021.9\pm0.1$ eV for the incorporated Zn. The first E_B value is similar to the values found in Ref. 13 for a Zn(S,O) layer with a ZnS/(ZnS+ZnO) ratio of ~80%. The position of the Zn $2p_{3/2}$ signal found on the etched samples is in good agreement with the binding energies ($E_B=1021.7-1022.0$ eV) found in the literature[41,42] for ZnS. In addition, the Zn $2p_{3/2}$ photoemission line of the etched samples corresponds, in terms of energetic position, quite well with that of a ZnS reference ($E_B^{ZnS}=1021.7\pm0.1$ eV) measured with the same XPS setup (taken from Ref. 13), which is also shown as dashed line in the upper part of Figs. 2(a) and 2(b). Furthermore, the Zn $L_3M_{45}M_{45}$ (^1G) XAES signal for the samples where the ZnS/Zn(S,O) buffer was etched away was found at a kinetic energy E_K of 989.5 ± 0.1 eV (not shown), which is again in good agreement with both the literature data for ZnS [$E_K^{lit}=988.2-989.9$ eV (Refs. 41 and 42)] and the measured data for a ZnS reference [$E_K^{ZnS}=989.5$ eV (Ref. 13)]. Thus, the incorporated Zn is bound to S. This supports the "incorporation" conclusion from above; because the Zn has to be somehow incorporated into the CIS absorber, otherwise—since it is bonded to S and due to the good solubility of ZnS in HCl (Ref. 40)—it would be etched away.

Since CIS is assumed to be HCl resistant as suggested by Liao and Rocket[20] the nevertheless decreased intensity of the Zn $2p_{3/2}$ XPS signal with increasing etching time can be explained by an increasingly leaching out of the incorporated Zn with extensively increased exposure time to the HCl_{aq} solution. For this explanation it is necessary to assume that most of the Zn stays close to or is incorporated into the absorber surface, respectively. Otherwise it could not be affected by wet-chemical processes. In order to clarify this issue we additionally performed depth-resolved photoelectron spectroscopy measurements on as-prepared (solid squares, black) and postannealed Zn(S,O)/ZnS/CIS samples (open circles, red) after 36 h HCl etching. Figure 3 shows the intensity of the Zn 3*d* photoemission line (normal-

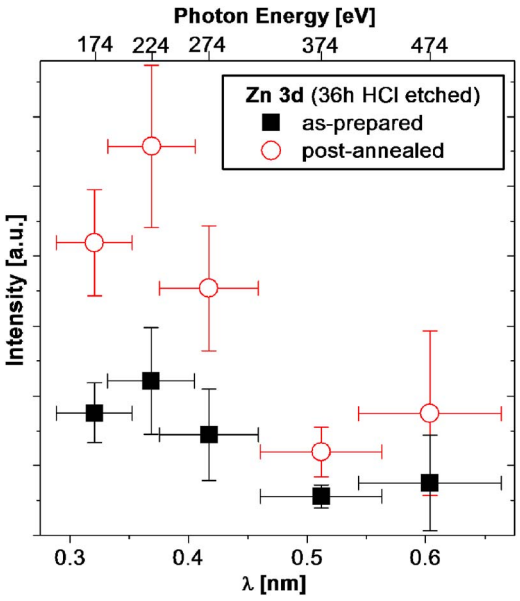

FIG. 3. (Color online) Intensity of the Zn 3*d* photoemission line (normalized to the corresponding excitation intensity, the respective cross section—taken from Ref. 43—and the transmission function of the electron analyzer) as a function of photoelectron escape depth of as-prepared (solid squares) and postannealed (open circles) buffer/CIS samples after 36 h HCl etching. The used exciting photon energies (174–474 eV) are shown on top.

ized to the corresponding excitation intensity, the respective cross section—taken from Ref. 43—and the transmission function of the electron analyzer) recorded at different photon energies (174–474 eV, as shown on top of Fig. 3). As a result of the increase of the exciting photon energy the kinetic energy of the Zn 3*d* photoelectrons is increasing and thus their IMFP is changing from ~0.61 to 1.15 nm. In consequence, the respective escape depth λ (abscissa of Fig. 3) increases (for $\varphi \approx 45°$) from ~0.32 to 0.60 nm with photon energy, probing the spatial distribution of the incorporated Zn in the upper region of the CIS absorber. As a result one can observe that for both the as-prepared as well as postannealed samples, the Zn 3*d* intensity is the highest for low photon energies, and thus low λ, showing that the major part of the incorporated Zn is indeed concentrated in the upper region of the CIS absorber regardless of sample treatment. Furthermore, Fig. 3 shows again that the postannealing enhances very well the Zn incorporation in to the surface-near region of the absorber, visualized by the higher intensity of the Zn 3*d* photoemission signal for this sample. Interestingly, we find the intensity maximum of the Zn 3*d* photoemission line for both measurement series at 0.37±0.04 nm, showing that the majority of the Zn is, in terms of spatial distribution, similarly extended into the absorber layer as the $[Zn_{(1-Z)},Cu_{2Z}]S$ interlayer is thick. In consequence, we interpret the observed Cu- and Zn-related intermixing as a CBD induced and heat-treatment promoted, spatially quite limited Cu–Zn ion exchange in the near buffer/absorber interface region. (However, a diffusion of minor amounts of Zn and/or Cu further in the "bulk" of the absorber and/or the buffer layer, respectively, cannot be excluded.) A similar result was found for the CBD-CdS/$Cu(In,Ga)(S,Se)_2$ interface, which was explained by a Cu–Cd ion exchange via the dominating

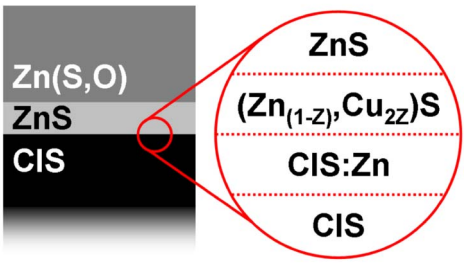

FIG. 4. (Color online) Illustration of the impact of the intermixing process across the Zn(S,O)/ZnS/CIS heterocontact on the buffer/absorber interface region in terms of composition.

complexes in the aqueous ammonia regime of the chemical bath.[44] In this context, one could speculate that the Zn, which is incorporated in the uppermost region of the CIS absorber, occupies liberated sites, which are left behind from the "out-leached" Cu, resulting in the observed formation of Zn–S bonds. In consequence, we rather term this modified region of the absorber CIS:Zn than suggesting the formation of a $[Cu_{(1-W)},Zn_{2W}]InS_4$ compound,[45] which would actually conform to our interpretation regarding the integration of the "out-leached" Cu in to the first monolayer(s) of the buffer forming a $[Zn_{(1-Z)},Cu_{2Z}]S$ interlayer. As a result of these conclusions, we have to modify the (compositional) picture of the buffer/absorber structure elaborated in Ref. 1 (shown in the left part of Fig. 4). The right part of Fig. 4 includes and summarizes the results regarding the intermixing at the CIS absorber and ZnS/Zn(S,O) bilayer buffer interface.

In order to evaluate whether the observed Cu–Zn ion exchange at the buffer/absorber interface is beneficial for the performance of the final solar cell, we discuss these findings in terms of their possible impacts on the electronic properties of the device in the following. First, we start with the suggested formation of a $[Zn_{(1-Z)},Cu_{2Z}]S$-like compound between buffer and absorber. In terms of band alignment at the buffer/absorber interface, the reduction of the high optical band gap energy of ZnS [E_g (ZnS)=3.68 eV, (Ref. 46)] by incorporation of Cu [E_g (Cu_2S)=1.20 eV (Ref. 47)] in this part of the bilayer buffer may be very well beneficial. The same may apply with regard to the conduction type (ZnS is *n* conducting and Cu_2S is *p* conducting) and thus to the position of the Fermi level E_F within the band gap. In consequence, not only E_g, but also E_F might be adjustable with the *Z* composition of the $[Zn_{(1-Z)},Cu_{2Z}]S$-like compound. On the other hand Cu–S phases are known to be conductive, short-circuiting the solar cell and thus deteriorating/killing the device, which is the reason for the necessary removal of the Cu_xS segregations prior to the buffer deposition by KCN etching (see Sec. II). However, in all these considerations one has to keep in mind that the suggested $[Zn_{(1-Z)},Cu_{2Z}]S$-like compound is very thin (i.e., in the range of approximately one monolayer).

Next, the possible impact of the Zn incorporation in the uppermost region of the CIS absorber on the performance of the final device is discussed. The bivalent Zn incorporated

into the absorber lattice on liberated sites of the "out-leached" univalent Cu (V_{Cu}^{-}), as suggested above, would cause an accumulation of positive charges at the buffer/absorber interface in terms of Zn_{Cu}^{+} states. The introduction of acceptorlike states on the surface of a *p*-conducting semiconductor as proposed here leads to a downward band bending at the surface. For the photogenerated electrons, which are minority charge carriers in the absorber, this means that they probably become majority charge carriers towards the defect-rich buffer/absorber interface. As a result, the recombination rate at the interface of the heterocontact will be reduced, improving the overall performance of the final solar cell device. In this terms also the beneficial effect of the heat treatment on the Zn(S,O)/ZnS/CIS samples, which results in a drastic performance enhancement of the respective solar cells, can be explained by the observed promotion of the Cu–Zn intermixing. A detailed analysis of the electronic properties of the heterointerface between CIS absorbers and ZnS/Zn(S,O) buffer bilayers before and after a heat treatment is currently under way.[48]

IV. SUMMARY AND CONCLUSION

The subject of this publication was to investigate the interface formation between wet-chemically-deposited ZnS/Zn(S,O) bilayer buffers and CIS absorbers. We have found indications that out-leached Cu from the absorber surface forms together with the educts in the chemical bath a $[Zn_{(1-Z)},Cu_{2Z}]$S-like interlayer between buffer and absorber. In return also an incorporation of Zn into the uppermost region of the CIS absorber was revealed, forming there Zn–S bonds. Both effects (Cu- and Zn-related intermixing at the buffer/absorber heterointerface) are strongly enhanced by postannealing the Zn(S,O)/ZnS/*interlayer*/CIS samples. Furthermore, it was determined that the major fraction of the Cu and Zn can be found quite close to the heterointerface in the buffer and absorber layer, respectively, regardless of sample treatment. Due to this limited ($\lesssim$0.4 nm) spatial extent, these "diffusion" mechanisms were interpreted as a CBD induced and heat-treatment promoted Cu–Zn ion exchange at the buffer/absorber interface.

In terms of solar cell performance the formation of a $[Zn_{(1-Z)},Cu_{2Z}]$S-like interlayer between buffer and absorber might be beneficial for the band alignment at the heterointerface due to the (via the *Z* composition) adjustable band-gap energy and Fermi-level position. Furthermore, the probable introduction of acceptorlike Zn_{Cu}^{+} states [and the resulting (enhanced) downward band bending towards the CIS surface] might also improve resulting solar cells devices. In this context, also the performance-enhancing impact of the heat treatment on resulting CIS solar cells with ZnS/Zn(S,O) buffer bilayer can be explained by the observed promotion of the Cu–Zn intermixing.

ACKNOWLEDGMENTS

Part of this work was funded by the European Commission under Nebules Project No. ENK6-2002-00664 as well as by the German BMBF (01SF0007) and BMWi (0329889). One of the authors (M.B.) is additionally grateful for partial sponsorship by the Emmy-Noether Program of the Deutsche Forschungsgemeinschaft (DFG).

[1] M. Bär *et al.*, J. Appl. Phys. **99**, 123503 (2006).
[2] K. Ramanathan *et al.*, Prog. Photovoltaics **11**, 225 (2003).
[3] M. A. Contreras, K. Ramanathan, J. AbuShama, F. Hasoon, D. L. Young, B. Egaas, and R. Noufi, Prog. Photovoltaics **13**, 209 (2005).
[4] T. Nakada and M. Mizutani, Jpn. J. Appl. Phys., Part 2 **41**, L165 (2002).
[5] A. Ennaoui, Can. J. Phys. **77**, 723 (1999).
[6] A. Ennaoui, S. Siebentritt, M. C. Lux-Steiner, W. Riedl, and F. Karg, Sol. Energy Mater. Sol. Cells **67**, 31 (2001).
[7] A. Ennaoui, W. Eisele, M. C. Lux-Steiner, T. P. Niesen, and F. Karg, Thin Solid Films **431–432**, 335 (2003).
[8] R. N. Bhattacharya, M. A. Contreras, and G. Teeter, Jpn. J. Appl. Phys., Part 2 **43**, L1475 (2004).
[9] M. A. Contreras, T. Nakada, M. Hongo, A. O. Pudov, and J. R. Sites, Proceedings of the Third World Conference on Photovoltaic Energy Conversion (WCPEC-3), Osaka, Japan, 2003, p. 570.
[10] K. Kushiya, M. Ohshita, I. Hara, Y. Tanaka, B. Sang, Y. Nagoya, M. Tachiyuki, and D. Yamase, Sol. Energy Mater. Sol. Cells **75**, 171 (2003).
[11] S. Neve, W. Bohne, J. Klaer, R. Klenk, and R. Scheer, Proceedings of the 17th European Photovoltaic Solar Energy Conference (Eu-PVSEC-17), Munich, Germany, 2001, p. 1102.
[12] L. L. Kazmerski, Technical Digest of the 12th International Photovoltaic Science and Engineering Conference (PVSEC-12), Cheju, South-Korea, 2001, p. 11.
[13] A. Ennaoui, M. Bär, J. Klaer, T. Kropp, R. Sáez-Araoz, and M. C. Lux-Steiner, Prog. Photovoltaics **14**, 499 (2006).
[14] S. D. Sartale, B. R. Sankapal, A. Ennaoui, and M. C. Lux-Steiner, Thin Solid Films **480–481**, 168 (2005).
[15] C. Heske *et al.*, Appl. Phys. Lett. **74**, 1451 (1999).
[16] J. Klaer, J. Bruns, R. Henninger, K. Siemer, R. Klenk, K. Ellmer, and D. Bräunig, Semicond. Sci. Technol. **13**, 1456 (1998).
[17] A. Ennaoui, T. Kropp, and M. C. Lux-Steiner, German Patent No. 10 2004 040 546.8-33 (pending).
[18] A. Ennaoui, M. Bär, J. Klaer, T. Kropp, R. Sáez-Araoz, and M. C. Lux-Steiner, Proceedings of the 20th European Photovoltaic Solar Energy Conference (EPVSEC-20), Barcelona, Spain, 2005, p. 1882.
[19] I. Lauermann *et al.*, Mater. Res. Soc. Symp. Proc. **763**, B4.5.1 (2003).
[20] D. Liao and A. Rocket, J. Appl. Phys. **93**, 9380 (2003).
[21] D. Briggs and M. P. Seah, *Practical Surface Analysis* (Wiley, New York, 1990), Vol. 1.
[22] S. Tanuma, C. J. Powell, and D. R. Penn, Surf. Interface Anal. **21**, 165 (1993).
[23] S. Tougaard, QUASES-IMP-TPP2M code for the calculation of the inelastic electron mean free path, Version 2.2; http://www.quases.com/
[24] R. Hunger *et al.*, presented at the Third World Conference on Photovoltaic Energy Conversion (WCPEC-3), Osaka, Japan, 2003.
[25] L. Weinhardt *et al.*, Appl. Phys. Lett. **82**, 571 (2003).
[26] S. M. Sze, *Physics of Semiconductor Device* (Wiley Interscience, New York, 1981), pp. 848–849.
[27] M. Bär *et al.*, The Fourth World Conference on Photovoltaic Energy Conversion (WCPEC-4), Waikoloa, USA, 2006.
[28] K. W. Boer, Survey of Semiconductor Physics (Van Nostrand Reinhold, New York, 1990), Vol. II.
[29] G. H. Hewig, F. Pfisterer, and H.-W. Schock, presented at the Fourth European Photovoltaic Solar Energy Conference (EPVSEC-4), Stresa, Italy, 1982.
[30] J.-F. Guillemoles, L. Kronik, D. Cahen, U. Rau, A. Jasenek, and H.-W. Schock, J. Phys. Chem. B **104**, 4849 (2000).
[31] M. Morkel, L. Weinhardt, B. Lohmüller, C. Heske, E. Umbach, W. Riedl, S. Zweigart, and F. Karg, Appl. Phys. Lett. **79**, 4482 (2001).
[32] L. Weinhardt, M. Morkel, Th. Gleim, S. Zweigart, F. Karg, C. Heske, and E. Umbach, Proceedings of the 17th European Photovoltaic Solar Energy Conference, Munich, Germany, 2001, p. 1261.
[33] L. Weinhardt *et al.*, Thin Solid Films **431–432**, 272 (2003).
[34] L. Weinhardt *et al.*, Appl. Phys. Lett. **86**, 062109 (2005).
[35] R. Herberholz *et al.*, Proceedings of the 26th IEEE Photovoltaic Specialists Conference (PVSC-26), Anaheim, CA, 1997, p. 323.
[36] R. Herberholz *et al.*, Eur. Phys. J.: Appl. Phys. **6**, 131 (1999).
[37] K. Ramanathan, H. Wiesner, S. Asher, D. Niles, R. N. Bhattacharya, J. Keane, M. A. Contreras, and R. Noufi, Proceedings of the Second World Conference on Photovoltaic Energy Conversion (WCPEC-2), Vienna, Austria, 1998, p. 477.

[38]W. Bohne, S. Lindner, and J. Röhrich, Nucl. Instrum. Methods Phys. Res. B **55**, 188 (2002).
[39]S. Lindner, W. Bohne, A. Jäger-Waldau, M. Ch. Lux-Steiner, J. Röhich, and G. Vogl, Thin Solid Films **403–404**, 432 (2002).
[40]*CRC Handbook of Chemistry and Physics*, edited by D. R. Lide (CRC, Boca Raton, FL, 2005); Internet Version 2005, http://www.hbcpnetbase.com
[41]L. S. Dake, D. R. Baer, and J. M. Zachara, Surf. Interface Anal. **14**, 71 (1989).
[42]NIST X-Ray Photoelectron Spectroscopy Database, NIST Standard Reference Database 20, Version 3.4; http://srdata.nist.gov/xps/
[43]J. J. Yeh and I. Lindau, At. Data Nucl. Data Tables **32**, 1 (1983).
[44]M. Bär, L. Weinhardt, C. Heske, H.-J. Muffler, M. Ch. Lux-Steiner, E. Umbach, and Ch.-H. Fischer, Prog. Photovoltaics **13**, 571 (2005).
[45]In close analogy a $CuCd_2InSe_4$ compound was suggested to be formed by Cd diffused into the upper region of $Cu(In,Ga)Se_2$ absorbers: T. Nakada, T. Mise, T. Kume, and A. Kunioka, presented at the Second World Conference on Photovoltaic Energy Conversion (WCPEC-2), Vienna, Austria, 1998.
[46]*Semiconductors*, Landold-Börnstein, Vol. III/41, supplement to Vol. III/17 (Springer-Verlag, Berlin, 1999), p. 22.
[47]S. Pakeva and K. Germanova, J. Phys. D **18**, 1371 (1985).
[48]M. Bär *et al.*, Appl. Phys. Lett. (to be published).